John von Neumann Institute for Computing

Boundary Effects in Microfluidic Setups

J. Harting, C. Kunert

published in

NIC Symposium 2008,
G. Münster, D. Wolf, M. Kremer (Editors),
John von Neumann Institute for Computing, Jülich,
NIC Series, Vol. **39**, ISBN 978-3-9810843-5-1, pp. 221-228, 2008.

http://www.fz-juelich.de/nic-series/volume39

Boundary Effects in Microfluidic Setups

J. Harting and C. Kunert

Institute for Computational Physics, University of Stuttgart
Pfaffenwaldring 27, 70569 Stuttgart, Germany
E-mail: jens@icp.uni-stuttgart.de

Due to large surface to volume ratios in microfluidic setups, the roughness of channel surfaces must not be neglected since it is not any longer small compared to the length scale of the system. In addition, the wetting properties of the wall have an important influence on the flow. Even though these effects are getting more and more important for industrial and scientific applications, the knowledge about the interplay of surface roughness and hydrophobic fluid-surface interaction is still very limited because these properties cannot be decoupled easily in experiments. We investigate the problem by means of lattice Boltzmann (LB) simulations of rough microchannels with tunable fluid-wall interaction. We introduce an "effective no-slip plane" at an intermediate position between peaks and valleys of the surface and observe how the position of the wall may change due to surface roughness and hydrophobic interactions. We find that the position of the effective wall, in the case of a Gaussian distributed roughness depends linearly on the width of the distribution. Further we are able to show that roughness creates a non-linear effect on the slip length for hydrophobic boundaries.

1 Introduction

The influence of the surface topologies and wetting behaviour of confining geometries in microfluidic systems is of great importance for the understanding of novel techniques using micro- or nanoscale geometries. Such systems allow to handle microliter or nanoliter quantities of liquid for production and analysis processes in the chemical and pharmaceutical industry, for scientific purposes or medical applications. Due to the small length scales in the system, the surface to volume ratio becomes more important. Assuming the surfaces to be perfectly flat and non-interacting is even on molecular scales an invalid assumption which can lead to large errors in experimental measurements. In this report we utilize lattice Boltzmann simulations to investigate the combined influence of roughness and wettability on the fluid flow. This leads to the question which boundary condition has to be applied at a surface in order to treat the surface topology properly. For more than a hundred years the no-slip boundary condition was successfully applied in engineering applications. Nevertheless, Navier[1] introduced a slip boundary condition

$$v(x=0) = \beta \frac{\partial v}{\partial x}$$

saying that the fluid velocity v at the boundary $x = 0$ is proportional to the velocity gradient $\frac{\partial v}{\partial x}$. The constant of proportionality is given by the slip length β. β depends on many parameters like the wettability, the surface roughness or fluid properties like the viscosity or molecular interactions. Therefore, it has to be seen as an empirical length that contains many to some extend unknown interactions. However, for simple liquids the measured slip lengths are commonly of the order of up to some tens of nanometers.

The influence of surface variations on the slip length β has been investigated by numerous authors. On the one hand roughness leads to higher drag forces and thus to no-slip on

macroscopic scales. Richardson showed that even if on a rough surface a full-slip boundary condition is applied, one can determine a flow speed reduction near the boundary resulting in a macroscopic no-slip assumption[2]. This was experimentally demonstrated by McHale and Newton[3]. On the other hand, roughness can cause pockets to be filled with vapour or gas nano bubbles leading to apparent slip[4]. Varnik et al.[5] applied the lattice Boltzmann (LB) method to show that even in small geometries rough channel surfaces can cause flow to become turbulent. Recently, Sbragaglia et al. applied the LB method to simulate fluids in the vicinity of microstructured hydrophobic surfaces[6]. In an approach similar to the one proposed by us, they modelled a liquid-vapour transition at the surface utilising the Shan-Chen multiphase LB model[7]. The authors were able to reproduce the behaviour of the capillary pressure as simulated by Cottin-Bizonne et al. using molecular dynamics (MD) simulations quantitatively[8].

During the last two years, we published a number of papers in which we presented a model to simulate hydrophobic surfaces with a Shan-Chen based fluid-surface interaction and investigated the behaviour of the slip length β[9,10]. We showed that the slip length β is independent of the shear rate, but depends on the pressure and on the concentration of surfactant added. Recently, we presented the idea of an effective wall for rough channel surfaces[11] and investigated the influence of different types of roughness on the position of the effective boundary. Further, we showed how the effective boundary depends on the distribution of the roughness elements and how roughness and hydrophobicity interact with each other[12]. In this report, we revise our previous achievements.

2 Simulation Method

We use a 3D LB model as presented in[13,9] to simulate pressure driven flow between two infinite rough walls that might be wetting or non-wetting. Since the method is well described in the literature we only shortly describe it here.

The lattice Boltzmann equation,

$$\eta_i(\mathbf{x}+\mathbf{c}_i, t+1) - \eta_i(\mathbf{x}, t) = \Omega_i,\ i = 0, 1, \ldots, b\,, \tag{1}$$

with the components $i = 0, 1, \ldots, b$, describes the time evolution of the single-particle distribution $\eta_i(\mathbf{x}, t)$, indicating the amount of quasi particles with velocity $\mathbf{c}_i$, at site $\mathbf{x}$ on a 3D lattice of coordination number $b = 19$, at time-step t.

We choose the Bhatnagar-Gross-Krook (BGK) collision operator

$$\Omega_i = -\tau^{-1}(\eta_i(\mathbf{x}, t) - \eta_i^{\mathrm{eq}}(\mathbf{u}(\mathbf{x}, t), \eta(\mathbf{x}, t))), \tag{2}$$

with mean collision time τ and equilibrium distribution η_i^{eq}[14]. We use the mid-grid bounce back boundary condition and choose $\tau = 1$ in order to recover the no-slip boundary conditions correctly. Interactions between the boundary and the fluid are introduced as mean field body force between nearest neighbours as it is used by Shan and Chen for the interaction between two fluid species[7,9]:

$$\mathbf{F}^{\mathrm{fluid}}(\mathbf{x}, t) \equiv -\psi^{\mathrm{fluid}}(\mathbf{x}, t) g_{\mathrm{fluid,\,wall}} \sum_{\mathbf{x}'} \psi^{\mathrm{wall}}(\mathbf{x}', t)(\mathbf{x}' - \mathbf{x})\,. \tag{3}$$

The interaction constant $g_{\mathrm{fluid,\,wall}}$ is set to 0.08 if not stated otherwise. The wall properties are given by the so-called wall density η_{wall}. This enters directly into the effective mass

$\psi^i = 1 - e^{-\frac{\eta^i}{\eta^0}}$, with the normalized mass $\eta^0 = 1$. With such a model we can simulate slip flow over hydrophobic boundaries with a slip length β of up to 5 in lattice units[9]. It was shown that this slip length is independent of the shear rate, but depends on the interaction parameters and on the pressure.

Here, we model Poiseuille flow between two infinite rough boundaries as shown in Fig. 1. Simulation lattices are 512 lattice units long in flow direction and the planes are

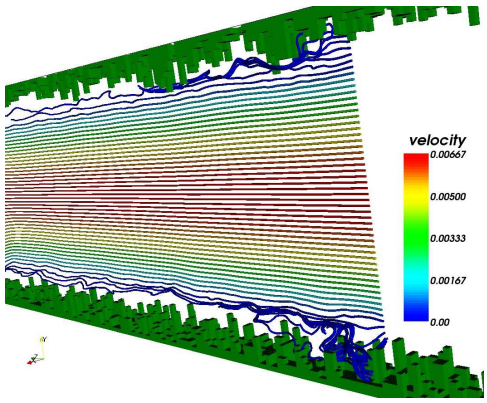

Figure 1. Poiseuille flow in between infinite rough boundaries. The colouring of the streamlines denotes the parabolic velocity profile, while close to the boundary the otherwise laminar streamlines become distorted.

separated by 128 sites between the lowest points of the roughness elements $h_{\min}$. Periodic boundary conditions are imposed in the remaining direction allowing us to keep the resolution as low as 16 lattice units. A pressure gradient is obtained by setting the pressure to fixed values at the in- and outflow boundary. The highest point of one plane gives the height of $h_{\max}$, while the average roughness is found to be R_a (see Fig. 2). In the case of symmetrical distributions $R_a = h_{\max}/2$.

The position of the effective boundary can be found by fitting the parabolic flow profile

$$v_z(x) = \frac{1}{2\mu}\frac{\partial P}{\partial z}\left[d^2 - x^2 - 2d\beta\right] \tag{4}$$

via the distance $2d = 2d_{\text{eff}}$. With β set to 0 we obtain the no-slip case. The viscosity μ and the pressure gradient $\frac{\partial P}{\partial z}$ are given by the simulation. To obtain an average value for d_{eff}, a sufficient number of individual profiles at different positions z are taken into account. The so found d_{eff} gives the position of the effective boundary and the effective height h_{eff} of the rough surface is then defined by $d_{\max} - d_{\text{eff}}$ (see Fig. 2).

3 Flow Along Rough Surfaces

Panzer et al. calculated the slip length β analytically for Poiseuille flow in the case of small cosine-shaped surface variations[15]. It is applicable to two infinite planes separated by a distance $2d$ being much larger than the highest peaks $h_{\max}$. Surface variations are

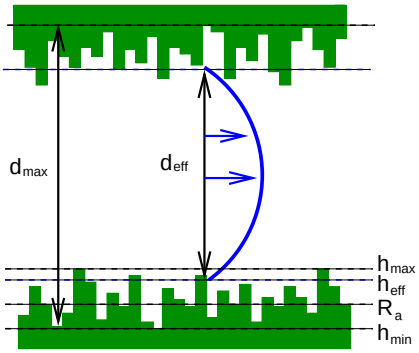

Figure 2. The effective boundary height h_{eff} is found between the deepest valley at h_{min} and the highest peak at h_{max} and corresponds to an effective channel width d_{eff}. For the utilized geometries the average roughness is equal to half the maximum height $R_a = h_{\mathrm{max}}/2$ (from[12]).

determined by peaks of height h_{max}, valleys at h_{min} and given by $h(z) = h_{\mathrm{max}}/2 + h_{\mathrm{max}}/2\cos(qz)$. Here, q is the wave number. Since the surfaces are separated by a large distance, the calculated slip length is equal to the negative effective boundary h_{eff} that is found to be

$$h_{\mathrm{eff}} = -\beta = \frac{h_{\mathrm{max}}}{2}\left(1 + k\frac{1 - \frac{1}{4}k^2 + \frac{19}{64}k^4 + \mathcal{O}(k^6)}{1 + k^2(1 - \frac{1}{2}k^2) + \mathcal{O}(k^6)}\right). \tag{5}$$

The first and k independent term shows the linear behaviour of the effective height h_{eff} on the average roughness $R_a = h_{\mathrm{max}}/2$. Higher order terms cannot easily be calculated analytically and are neglected. Thus, Eq. 5 is valid only for $k = qh_{\mathrm{max}}/2 \ll 1$. However, for realistic surfaces, k can become substantially larger than 1 causing the theoretical approach to fail. Here, only numerical simulations can be applied to describe arbitrary boundaries. In Fig. 3 the normalized effective height h_{eff}/R_a obtained from our simulations is plotted versus k for cosine shaped surfaces with $h_{\mathrm{max}}/2 = k = 1, \frac{1}{2}, \frac{1}{3}$ (symbols). The line is given by the analytical solution of Eq. 5. For $k < 1$ the simulated data agrees within 2.5% with Panzer's prediction. However, for $k = 1$ a substantial deviation between numerical and analytical solutions can be observed because Eq. 5 is valid for small k only. In the case of large $k > 1$, the theory is not able to correctly reproduce the increase of β with increasing h_{max} anymore. Instead, $2\beta/h_{\mathrm{max}}$ becomes smaller again due to missing higher order contributions in Eq. 5. Our simulations do not suffer from such limitations allowing us to study arbitrarily complex surface geometries[11].

We showed that the position of the effective boundary height is depending on the shape of the roughness elements, i.e., for strong surface distortions it is between 1.69 and 1.90 times the average height of the roughness $R_a = h_{\mathrm{max}}/2$[11]. By adding an additional distance between roughness elements, h_{eff} decreases slowly, so that the maximum height is still the leading parameter. We are also able to simulate flow over surfaces generated from AFM data of gold coated glass used in microflow experiments by O.I. Vinogradova and G.E. Yakubov[16]. We find that the height distribution of such a surface is Gaussian and that a randomly arranged surface with a similar distribution gives the same result for the position of the effective boundary although in this case the heights are not correlated. We

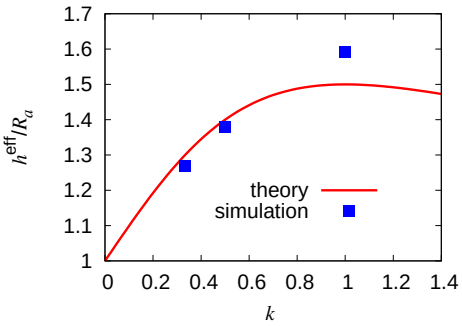

Figure 3. Effective height h_{eff} normalized by the average roughness R_a versus $k = h_{\max}/2q$ for a cosine geometry. Symbols denote numerical data and the line is given by Eq. 5. For $k > 1$ the theory fails simulations are still valid in this regime (from[12]).

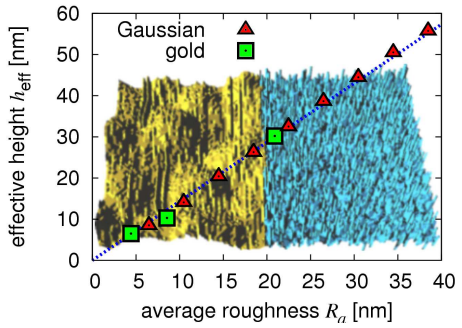

Figure 4. Simulated h_{eff} versus R_a for gold coated glass and a randomly generated surface with Gaussian distributed heights. The background image shows the gold surface (left) and the artificially generated structure (right)[11].

can set the width of the distribution σ and the average height R_a. By scaling σ with R_a we obtain geometrically similar geometries. This similarity is important because the effective height h_{eff} scales with the average roughness in the case of geometrical similarity[11] (see Fig. 4). As an extension of our previous work, we investigate Gaussian distributed heights with different widths σ. In Fig. 5 the effective height h_{eff} is plotted over the average height R_a for $0.054 < \sigma/R_a < 0.135$. The height of the effective wall depends linearly on σ in the observed range as can be seen in the inset[12]. The effective height h_{eff} ranges from $1.15R_a$ to $1.45R_a$. These values are lower than the effective heights for an equally distributed roughness ($1.84R_a$).

4 Wettability and Roughness

We also investigate how roughness and the surface wettability act together by performing simulations with rough channels to which we assign a fluid-wall interaction as given in the

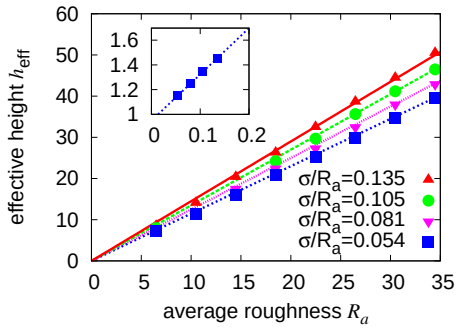

Figure 5. Effective height h_{eff} over average roughness R_a for Gaussian distributed height elements with different width of the distribution σ. Symbols are the simulation results, lines are a linear fit to the data. The inset shows the linear dependence of the effective height on σ[12].

introduction (Eq. 3, η_{wall}= 0.5, 1, and 5). For perfectly smooth surfaces we determine β to be 0.65, 1.13, and 1.3. Fig. 6 depicts the effective height of rough hydrophobic walls versus R_a. For $R_a > 4$ we find a linear dependence between R_a and h_{eff}. The slope for different η_{wall} varies because the fluid-surface interaction does not cause a simple offset on the effective height h_{eff}. Instead, non-linear effects are playing a role.

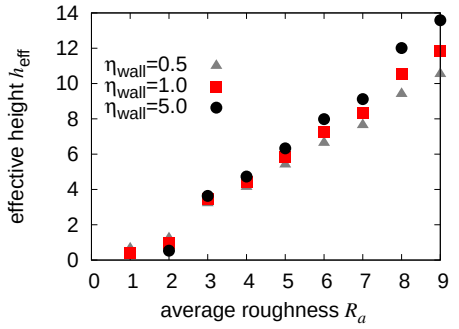

Figure 6. Effective height h_{eff} versus average roughness R_a with different fluid-wall interaction constant η_{wall}. The position of the effective height h_{eff} spreads wider for higher R_a, because larger roughness increases the fluid-wall interaction[12].

To decouple the effects of roughness and wettability we determine the slip length by setting the effective distance d_{eff} in equation (4) to the effective distance for a rough no-slip wall. We then fit the corresponding velocity profile via β. In Fig. 7 we can see that the slip length β for the strong fluid-wall interaction ($\eta^{\mathrm{wall}} = 5$) first decreases with the average roughness and then rises. For a lower interaction, the slip length is constantly growing and leads to an increase of the slip length for weak fluid wall interaction ($\eta_{\mathrm{wall}} = 0.5$) by a factor of more than three. There are two counteracting effects in this system and their interplay can explain the observed behaviour. The decrease of the slip length β is due to an increased friction near the boundary at moderate roughness. The increase has its

reason in the reduced pressure near the hydrophobic rough surface, so that the fluid "feels" a smoothed effective surface. For a more detailed study on superhydrophobic surfaces, the strong surface variation as well as the liquid-gas transitions have to be taken into account. This is ongoing work and will be reported on in the future.

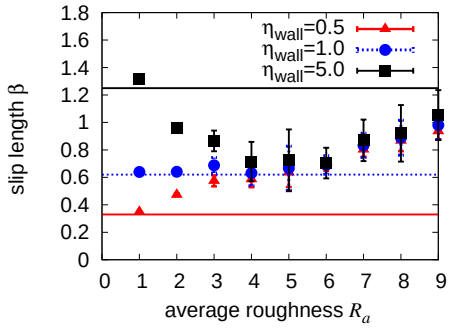

Figure 7. Slip length β over average roughness R_a for equally distributed height elements with different fluid-wall interaction $\eta_{\mathrm{wall}} = 0.5,\ 1.0,\ 5.0$. The position of the effective height h_{eff} is chosen as the value for a non-interacting wall. The lines show the slip lengths for smooth boundaries. Error bars show the standard deviation of results from four different random surfaces[12].

5 Conclusion

In this report we summarized our work on fluid flow along rough and hydrophobic surfaces which has been performed during the last two years. We demonstrated that there is a linear dependence of the effective height on the average roughness and that the average height scales linearly with the width of the distribution of heights σ. We successfully applied our simulations to experimental data and showed that neglecting roughness can lead to substantial errors in experimental measurements. Currently, we investigate the interplay between roughness and hydrophobic fluid-wall interactions and presented preliminary results. They show that there exist non-linear interactions between roughness and hydrophobicity leading to an increase of the slip length and eventually to superhydrophobic effects.

Acknowledgments

We thank the John von Neumann Institute for Computing, Jülich for providing the computing time and technical support for the presented work. This work was financed within the DFG priority program "nano- and microfluidics" and by the "Landesstiftung Baden-Württemberg".

References

1. C.L.M.H. Navier, *Mémoire sur les lois du mouvement de fluids*, Mem. Acad. Sci. Ins. Fr., **6**, 389, 1823.

2. S. Richardson, *On the no-slip boundary condition*, J. Fluid Mech., **59**, 707, 1973.
3. G. McHale and M.I. Newton, *Surface roughness and interfacial slip boundary condition for quarzcrystal microbalances*, J. Appl. Phys., **95**, 373, 2004.
4. P. Joseph, C. Cottin-Bizonne, J. M. Benoi, C. Ybert, C. Journet, P. Tabeling, and L. Bocquet, *Slippage of water past superhydrophobic carbon nanotube forest in microchannels*, Phys. Rev. Lett., **97**, 156104, 2006.
5. F. Varnik, D. Dorner, and D. Raabe, *Roughness-induced flow instability: A lattice Boltzmann study*, J. Fluid Mech., **573**, 191, 2006.
6. M. Sbragaglia, R. Benzi, L. Biferale, S. Succi, and F. Toschi, *Surface roughness-hydrophobicity coupling in micro and nanochannel flows*, Phys. Rev. Lett., **97**, 204503, 2006.
7. X. Shan and H. Chen, *Lattice boltzmann model for simulating flows with multiple phases and components*, Phys. Rev. E, **47**, 1815, 1993.
8. C. Cottin-Bizone, C. Barentin, E. Charlaix, L. Bocquet, and J.L. Barrat, *Dynamics of simple liquids at heterogeneous surfaces: molecular dynamics simulations and hydrodynamic description*, Eur. Phys. J. E, **15**, 427, 2004.
9. J. Harting, C. Kunert, and H.J. Herrmann, *Lattice Boltzmann simulations of apparent slip in hydrophobic microchannels*, Europhys. Lett., pp. 328–334, 2006.
10. C. Kunert and J. Harting, *On the effect of surfactant adsorption and viscosity change on apparent slip in hydrophobic microchannels*, Progress in CFD, **in press**, 2007.
11. C. Kunert and J. Harting, *Roughness induced apparent boundary slip in microchannel flows*, Phys. Rev. Lett., **99**, 176001, 2007.
12. C. Kunert and J. Harting, *Simulation of fluid flow in hydrophobic rough micro channels*, Submitted for publication, **arXiv:0709.3966**, 2007.
13. J. Harting, M. Harvey, J. Chin, M. Venturoli, and P. V. Coveney, *Large-scale lattice Boltzmann simulations of complex fluids: advances through the advent of computational grids*, Phil. Trans. R. Soc. Lond. A, **363**, 1895–1915, 2005.
14. S. Succi, *The Lattice Boltzmann Equation for Fluid Dynamics and Beyond*, Oxford science publications, 2001.
15. P. Panzer, M. Liu, and D. Einzel, *The effects of boundary curvature on hydrodynamic fluid flow:Calculation of slip lengths*, Int. J. mod. Phys. B, **6**, 3251, 1992.
16. O.I. Vinogradova and G.E. Yakubov, *Surface roughness and hydrodynamic boundary conditions*, Phys. Rev. E, **73**, 045302(R), 2006.